



The *MYC* mRNA 3'-UTR couples RNA polymerase II function to glutamine and ribonucleotide levels

Francesca R Dejure^{1,†}, Nadine Royle^{2,†}, Steffi Herold¹, Jacqueline Kalb¹, Susanne Walz³, Carsten P Ade¹, Guido Mastrobuoni², Jens T Vanselow⁴, Andreas Schlosser⁴, Elmar Wolf⁵, Stefan Kempa^{2,*}  & Martin Eilers^{1,**} 

Abstract

Deregulated expression of *MYC* enhances glutamine utilization and renders cell survival dependent on glutamine, inducing “glutamine addiction”. Surprisingly, colon cancer cells that express high levels of *MYC* due to WNT pathway mutations are not glutamine-addicted but undergo a reversible cell cycle arrest upon glutamine deprivation. We show here that glutamine deprivation suppresses translation of endogenous *MYC* via the 3'-UTR of the *MYC* mRNA, enabling escape from apoptosis. This regulation is mediated by glutamine-dependent changes in adenosine-nucleotide levels. Glutamine deprivation causes a global reduction in promoter association of RNA polymerase II (RNAPII) and slows transcriptional elongation. While activation of *MYC* restores binding of *MYC* and RNAPII function on most promoters, restoration of elongation is imperfect and activation of *MYC* in the absence of glutamine causes stalling of RNAPII on multiple genes, correlating with R-loop formation. Stalling of RNAPII and R-loop formation can cause DNA damage, arguing that the *MYC* 3'-UTR is critical for maintaining genome stability when ribonucleotide levels are low.

Keywords 3'-UTR; glutamine; *MYC*; RNA polymerase II

Subject Categories Cancer; Metabolism; Transcription

DOI 10.15252/embj.201796662 | Received 3 February 2017 | Revised 16 March 2017 | Accepted 16 March 2017 | Published online 13 April 2017

The EMBO Journal (2017) 36: 1854–1868

See also: **CV Dang** (July 2017)

Introduction

Deregulated and enhanced expression of one of three *MYC* genes (*MYC*, *MYCN*, and *MYCL*) is observed in multiple tumor entities, and inhibition of *MYC* function can selectively eradicate tumor cells

(Soucek *et al*, 2008; Dang, 2012; Annibali *et al*, 2014). *MYC* proteins are transcription factors that broadly bind to promoters and enhancers with an open chromatin structure (Wolf *et al*, 2014; Kress *et al*, 2015). Enhanced expression of *MYC* proteins promotes cell growth and cell proliferation in tissue culture and *in vivo*, suggesting that promoting both processes is a critical oncogenic function of *MYC* (Barna *et al*, 2008; Dang, 2012).

To promote growth and proliferation, *MYC* proteins exert profound effects on many aspects of cell metabolism (Carroll *et al*, 2015). *MYC* regulates multiple genes involved in glucose utilization and thereby increases the aerobic use of glucose and its conversion into lactate (Shim *et al*, 1997; Doherty *et al*, 2014). Similarly, *MYC* increases uptake of glutamine and its flux into downstream metabolic pathways via regulation of genes encoding glutamine transporters (Wise *et al*, 2008), enzymes of glutamine metabolism (Eberhardy & Farnham, 2001; Bott *et al*, 2015), and microRNAs that control expression of these genes (Gao *et al*, 2009). Collectively, these changes promote the biosynthesis of macromolecules and enable cells to avoid apoptosis (Hsu & Sabatini, 2008).

These observations have led to the hypothesis that targeting alterations in cell metabolism is a potentially universal strategy to selectively eradicate *MYC*-driven tumor cells (Dang, 2011; Gouw *et al*, 2016). This notion is supported by observations that *MYC*-driven tumor cells can be “glutamine-addicted”, a term that describes the dependency of *MYC*-driven tumor cells on an external supply of glutamine for survival (Wise *et al*, 2008). Glutamine addiction of *MYC*-driven tumor cells has been observed in multiple experimental systems, both in tissue culture and *in vivo* (Yuneva *et al*, 2007, 2012; Gao *et al*, 2009; Qing *et al*, 2012; Xiang *et al*, 2015). The concept has spurred the development of glutaminase inhibitors for tumor therapy. One of these inhibitors is in current clinical trials, using amplification of *MYC* as a marker for patient stratification (ClinicalTrials.gov: NCT02071862).

Somewhat paradoxically, a parallel series of experiments has demonstrated that expression of *MYC* is sensitive to stress,

1 Theodor Boveri Institute and Comprehensive Cancer Center Mainfranken, Biocenter, University of Würzburg, Würzburg, Germany

2 Berlin Institute for Medical Systems Biology, Max-Delbrück-Center for Molecular Medicine, Berlin, Germany

3 Comprehensive Cancer Center Mainfranken, Core Unit Bioinformatics, Biocenter, University of Würzburg, Würzburg, Germany

4 Mass Spectrometry and Proteome Research, Rudolf-Virchow-Center, University of Würzburg, Würzburg, Germany

5 Cancer Systems Biology, Biocenter, University of Würzburg, Würzburg, Germany

*Corresponding author. Tel: +49 3094063033; E-mail: stefan.kempa@mdc-berlin.de

**Corresponding author. Tel: +49 9313184111; E-mail: martin.eilers@biozentrum.uni-wuerzburg.de

†These authors contributed equally to this work

including metabolic stress, in many experimental systems. For example, translation of MYC is regulated by internal ribosomal entry sites that are present in the 5'-UTR (Stoneley *et al*, 2000; Wiegner *et al*, 2015). Conversely, the 3'-UTR of MYC is targeted by a large number of microRNAs, including LET-7 (Kim *et al*, 2009), the miR-34 family (Cannell *et al*, 2010; Christoffersen *et al*, 2010; Kress *et al*, 2011), miR-24 (Lal *et al*, 2009), miR-17-19b (Mihailovich *et al*, 2015), and others. Expression of these miRNAs (in particular the miR-34 family) is regulated by FoxO and p53 transcription factors, coupling endogenous MYC expression to the cellular energy status and stress-dependent signals (He *et al*, 2007; Hermeking, 2007; Cannell *et al*, 2010; Kress *et al*, 2011; Zheng *et al*, 2011).

Many of the experimental strategies used to demonstrate glutamine addiction use ectopic expression of MYC as model, and most transgenes used do not contain the 3'-UTR. However, the 3'-UTR is not mutated in human tumors, suggesting that metabolic controls that impinge on MYC expression via the 3'-UTR may have been overlooked. To address this question, we studied the glutamine dependence of colon carcinoma cells, since colon carcinomas universally express high levels of MYC due to mutations in the WNT signaling pathway (He *et al*, 1998; van de Wetering *et al*, 2002; Sansom *et al*, 2007).

Results

Glutamine deprivation induces a reversible S-phase arrest in colon carcinoma cells

In order to test whether colon cancer cells depend on an external supply of glutamine for survival, we cultured HCT116 carcinoma cells, which express high levels of MYC due to an activating point mutation in the beta-catenin gene (Polakis, 1999), in complete medium, in medium lacking glutamine, or in medium lacking glucose. Deprivation of either glutamine or glucose suppressed growth of HCT116 to a varying extent (Fig 1A). FACS analyses of annexin V/propidium iodide-stained cells after 36 h of nutrient deprivation showed that depletion of glucose led to a large increase in both early and late apoptotic cells, whereas deprivation of glutamine led to only a moderate increase in apoptosis (Fig 1B). Parallel FACS analyses of cells labeled with BrdU after 15 h of glutamine deprivation provided little evidence for apoptosis but instead showed a cell cycle arrest predominantly in late S-phase (Fig 1C). Re-addition of glutamine restored BrdU incorporation and promoted rapid cell cycle progression (Fig 1C and D). We concluded that glutamine deprivation suppresses growth of HCT116 cells primarily via inducing a reversible cell cycle arrest.

HCT116 express approximately 300,000–600,000 molecules of MYC per cell, which is about 10- to 20-fold higher than levels expressed in several non-transformed proliferating cell lines (Lorenzin *et al*, 2016). The comparison with U2OS cells expressing doxycycline-inducible alleles of MYC showed that these levels are sufficient to suppress colony formation and induce apoptosis in U2OS cells (Walz *et al*, 2014; Lorenzin *et al*, 2016). To understand why HCT116 cells undergo a reversible cell cycle arrest upon glutamine deprivation, we determined endogenous MYC levels by immunoblotting. These experiments showed that glutamine deprivation suppressed expression of MYC (Fig 1E). Titration of glutamine showed that the EC₅₀ value for MYC was approximately 0.5 mM,

which is slightly below glutamine concentrations in human plasma (0.6–0.8 mM; Felig *et al*, 1970), suggesting that glutamine availability in tissues is a physiologically relevant regulator of MYC expression (Fig 1E). In contrast, deprivation of glucose did not significantly alter MYC expression (Appendix Fig S1A). Re-addition of glutamine after 15 h of deprivation rapidly restored MYC expression ($t_{1/2}$ = 13.5 min; Fig 1F). Similarly, glutamine deprivation suppressed MYC expression and cell growth in four additional colon carcinoma cell lines (Appendix Fig S1B). We concluded that expression of MYC is tightly and rapidly regulated by extracellular glutamine levels in colon carcinoma cells.

Glutamine regulates MYC expression via the 3'-UTR

The activating mutation in beta-catenin leads to deregulated and constitutive expression of MYC mRNA in HCT116 cells (He *et al*, 1998). In response to glutamine deprivation, we observed a moderate further increase in MYC mRNA levels, which is due to a well-known negative feedback loop, in which MYC proteins autosuppress transcription of MYC (Penn *et al*, 1990; Appendix Fig S1B and C). MYC proteins are rapidly turned over by the ubiquitin–proteasome system, and one of the critical ubiquitin ligases, FBXW7, recognizes a phosphodegron that is phosphorylated by MAP kinases and GSK3, suggesting that glutamine-dependent changes in growth factor-dependent signaling may regulate MYC via FBXW7 (Sears *et al*, 2000; Welcker *et al*, 2004). However, determination of MYC levels after addition of cycloheximide in medium containing either 2 mM or 0.5 mM glutamine did not reveal a change in MYC stability (Fig EV1A; note that MYC levels in the complete absence of glutamine were too low to reliably determine stability). Furthermore, the abundance of other short-lived proteins such as c-JUN or MCL1 that are turned over by FBXW7 and carry a similar phosphodegron did not alter in response to glutamine deprivation (Fig EV1B). Finally, the low levels of MYC in the absence of glutamine were not significantly elevated by addition of the proteasome inhibitor, MG132 (Fig EV1C). In contrast, pulse-labeling using ³⁵S-methionine showed that glutamine deprivation essentially shut down translation of MYC and that re-addition of glutamine restored translation (Fig 2A). We concluded that translation of MYC is controlled by glutamine levels.

Glutamine activates mTORC1, which is a potent activator of translation of MYC, suggesting that activation of mTORC1 may account for the regulation of MYC levels by glutamine (West *et al*, 1998; Nicklin *et al*, 2009; Duran *et al*, 2012). To test this hypothesis, we depleted and re-added glutamine to HCT116 as before in the presence of the mTORC1 inhibitor rapamycin, and in the presence of OSI-027, an inhibitor of both mTORC1 and mTORC2 (Bhagwat *et al*, 2011). Consistent with the published data, glutamine deprivation decreased mTORC1 activity as witnessed by a reduction in phosphorylation of 4EBP1 at T70 and of p70S6 kinase at T389; re-addition of glutamine strongly stimulated phosphorylation (Fig EV1D and E). Addition of rapamycin blunted phosphorylation of 4EBP1 and attenuated phosphorylation of S6 kinase at T389, demonstrating that it is effective in inhibiting mTORC1. Importantly, rapamycin did not affect downregulation of MYC levels upon glutamine deprivation and only moderately attenuated induction upon re-addition of glutamine (Fig EV1D). Identical results were obtained with OSI-027 (Fig EV1E). Starvation for two other amino acids, methionine and leucine, also reduced MYC levels and TORC

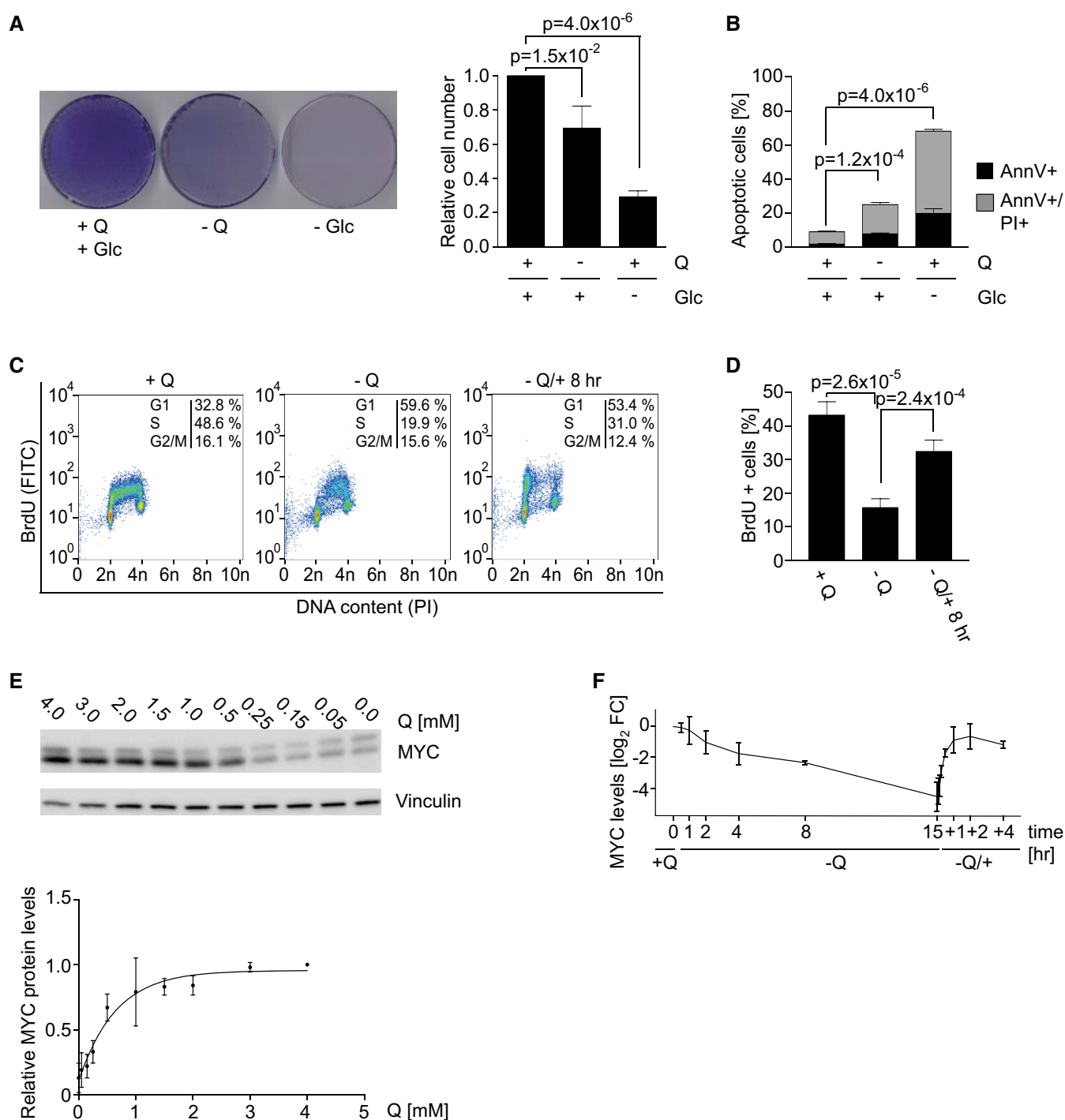


Figure 1. Effects of glutamine starvation on growth and MYC levels in HCT116 cells.

- A** Effects of glucose (Glc) or glutamine (Q) deprivation on cell growth. Colonies were stained with crystal violet after starvation for 36 h. Quantification of three independent experiments is shown on the right. Results represent mean \pm SD. *P*-values were calculated using Student's *t*-test.
- B** FACS analysis showing the percentage of early apoptotic (AnnV+; Ann: annexin) and late apoptotic (AnnV+/PI+; PI: propidium iodide) HCT116 cells after 36 h of starvation. Results represent mean \pm SD (*n* = 3). *P*-values were calculated for all apoptotic cells using Student's *t*-test.
- C** FACS analysis of BrdU/PI-stained cells. Cells were grown in complete medium or medium without glutamine for 15 h. Where indicated, glutamine was re-added for 8 h. Cells were labeled with BrdU for 1 h.
- D** Quantification of BrdU-positive cells. Results represent mean \pm SD (*n* = 4). *P*-values were calculated using Student's *t*-test.
- E** Top: Immunoblot documenting MYC protein levels in HCT116 cells cultured in medium containing the indicated amounts of glutamine for 24 h (*n* = 3). Bottom: Quantification of three independent experiments. Each point represents mean \pm SD. Curve fitting was performed using a sigmoidal dose-response equation.
- F** Time course of MYC protein levels in cells starved for 15 h, followed by re-addition of glutamine at the indicated time points. Each value was normalized to +Q at time point 0. Results represent mean \pm SD (*n* = 4).

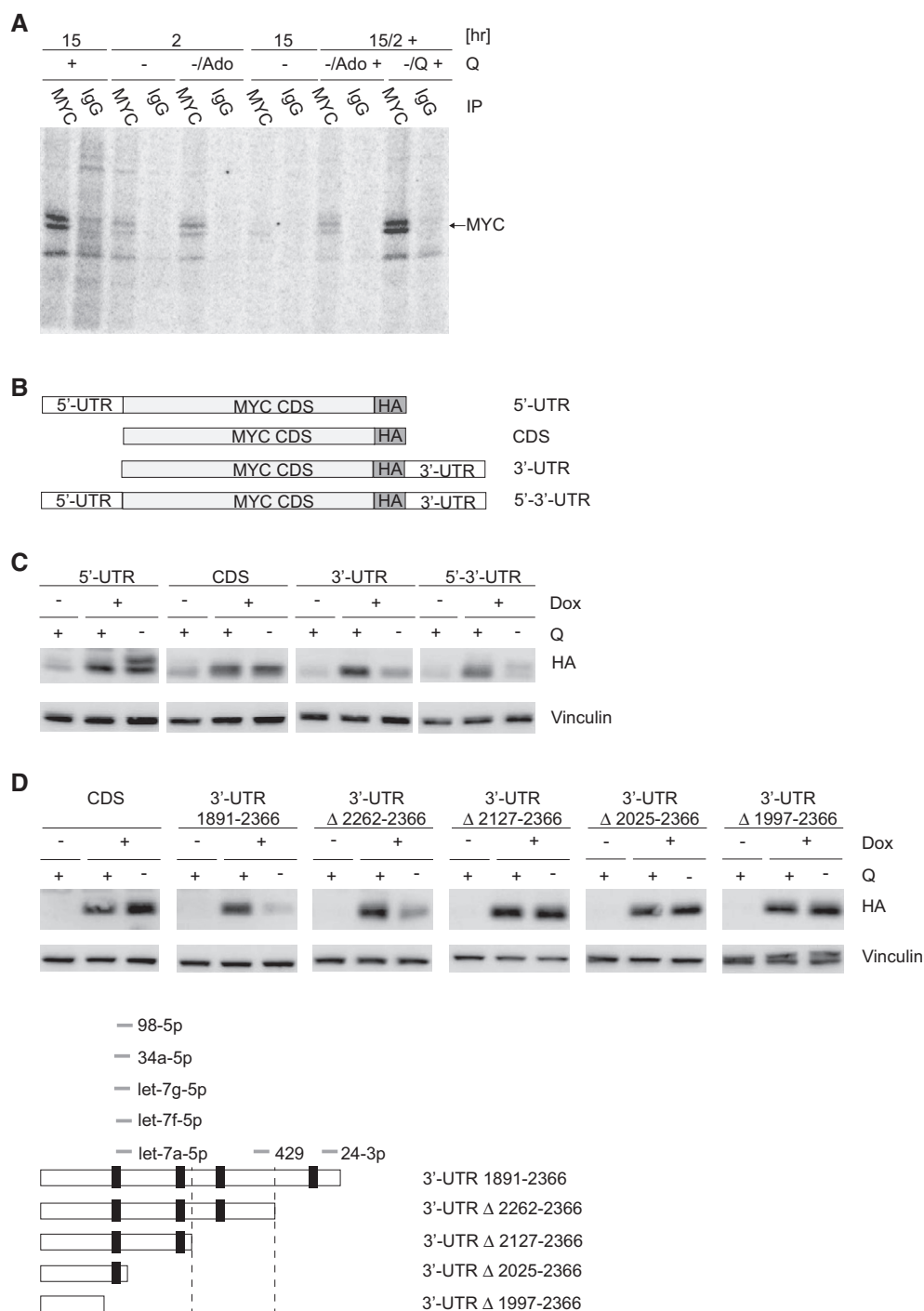


Figure 2. The 3'-UTR of MYC mediates the response to glutamine.

A 35 S-methionine labeling of HCT116 followed by immunoprecipitation with α -MYC or control antibodies. Glutamine starvation was performed for 2 or 15 h. Where indicated, adenosine (Ado, 150 μ M) was supplemented or re-added to the medium after starvation. The arrow indicates the specific MYC band detected by autoradiography ($n = 2$).

B Diagram depicting the doxycycline (Dox)-inducible MYC constructs used for lentiviral infection of HCT116 cells. All constructs contain a carboxy-terminal HA-tag. CDS, coding sequence.

C Immunoblot documenting levels of ectopically expressed MYC. Glutamine starvation was started after 2 h of Dox-mediated induction and maintained for 15 h in the presence of Dox. Exogenous MYC levels were detected by α -HA immunoblot ($n = 3$).

D Top: Immunoblot showing levels of exogenous MYC. The experiment was performed as in (C), using Dox-inducible MYC constructs ($n = 3$). CDS and 3'-UTR constructs are described in (A). Four 3'-UTR deletions are depicted at the bottom. Numbers refer to the annotated MYC sequence NM_002467.4. Vertical dashed lines indicate the region responsible for MYC regulation. Black boxes indicate the position of the AU-rich elements (AUUUA sequences) present in MYC 3'-UTR. Gray dashes indicate the predicted binding sites of miRNAs (shown in Appendix Fig S3).

activity, consistent with known effects of amino acid availability on mTORC1 (Fig EV1F; Nicklin *et al*, 2009). Importantly, re-addition of either amino acid to depleted cells restored phosphorylation of S6K by mTORC1, but, unlike glutamine, had no rapid effect on MYC levels (Fig EV1F). Finally, neither siRNA-mediated depletion of raptor or rictor abolished regulation of MYC levels in response to glutamine starvation (Appendix Fig S2). We concluded that changes in mTORC activity do not account for regulation of MYC by glutamine. We also speculated that stress due to glutamine deprivation might induce p53 to regulate MYC expression, but experiments using P53-deficient HCT116 cells established that p53 is not required for regulation of MYC levels by glutamine (Fig EV1G).

Multiple stress-response pathways impinge on MYC via the 5'- and 3'-UTR (see Introduction), prompting us to map the elements that respond to glutamine deprivation on the MYC mRNA. To do so, we stably expressed doxycycline-inducible alleles of HA-tagged MYC from constructs that encompass either the entire MYC mRNA, only the coding sequence or the coding sequence and the 5'-UTR or the 3'-UTR, respectively, using lentiviral transduction (Fig 2B). In order not to alter cell physiology or compete out any possible repressive factors, we chose constructs that express low levels of MYC relative to endogenous levels for these experiments. Inclusion of the 5'-UTR led to the pronounced appearance of a second band with reduced mobility in MYC immunoblots, but not to downregulation of MYC in glutamine-starved cells (Fig 2C). Previous work has established that a CUG codon upstream of the canonical AUG codon in the 5'-UTR of MYC can initiate translation (Hann *et al*, 1988). Mutation of the CUG confirmed that glutamine deprivation stimulated the use of this codon (Fig EV2A). In contrast, inclusion of the 3'-UTR led to robust downregulation of MYC protein in the absence of glutamine (Figs 2C and EV2B). A deletion series showed that the glutamine-responsive region is between nucleotides 2,127 and 2,366 of the MYC mRNA (Fig 2D). qRT-PCR assays showed a minor decrease in steady-state mRNA levels of constructs containing the 3'-UTR in the absence of glutamine, suggesting that changes in mRNA stability contribute to the effect on MYC translation (Fig EV2C; note that the constructs used in this experiment are not subject to MYC-dependent auto-suppression). We concluded that glutamine deprivation inhibits MYC translation via the 3'-UTR.

The 3'-UTR of MYC protects tumor cells from glutamine addiction

It is possible that the low level of apoptosis observed in HCT116 cells upon glutamine deprivation is due to the presence of anti-apoptotic mutations in these tumor cells rather than to downregulation of MYC. To test this possibility, we stably expressed a MYC-ER protein in HCT116 cells and measured cell growth and apoptosis in response to glutamine deprivation (Fig 3A). Addition of 4-hydroxytamoxifen to activate MYC-ER strongly suppressed colony formation (Fig 3B and C) and induced apoptosis (Fig 3D) upon glutamine deprivation. Both observations recapitulate previous work (Yuneva *et al*, 2007). To test the effect of the 3'-UTR, we expressed a MYC-ER construct that contains the 3'-UTR. As shown above for wild-type MYC, expression of MYC-ER-3'-UTR was attenuated in the absence of glutamine (Fig 3A). This led to enhanced colony formation of glutamine-starved cells (Fig 3B and

C). In addition, inclusion of the 3'-UTR reduced apoptosis upon glutamine deprivation, arguing that this contributes to the restoration of colony formation in cells expressing MYC-ER-3'-UTR (Fig 3D). We concluded that the 3'-UTR of MYC suppresses glutamine addiction of colon cancer cells.

The 3'-UTR of MYC responds to cellular adenosine levels

A major function of glutamine is to supply intermediates for the TCA cycle after its conversion to glutamate and α -ketoglutarate (Fig EV3A). Consistently, glutamine deprivation led to a rapid decrease in steady-state levels of glutamate and the TCA cycle intermediates α -ketoglutarate, fumarate, and malate (Fig 4A). In addition, glutamine deprivation reduced steady-state levels of ornithine and putrescine, indicating an overall reduction in nitrogen metabolism (Fig EV3B). In contrast, glutamine starvation had little effect on steady-state levels of several intermediates of glycolysis (Fig 4A). Glutamine also contributes to redox homeostasis, since glutamate is incorporated into glutathione and since glutamate dehydrogenase contributes to the pool of reducing equivalents (Fig EV3A), and we observed an increase in levels of reactive oxygen species upon glutamine deprivation (Fig EV3C). Finally, glutamine donates amino groups for the synthesis of pyrimidine and purine nucleotides and levels of multiple nucleotides decreased after glutamine deprivation (Fig 4B).

To determine which—if any—of these changes mediates regulation of MYC, we performed re-addition experiments of glutamine-derived metabolites. Addition of *N*-acetyl-cysteine, glutamate, and membrane-permeable forms of α -ketoglutarate, succinate, and pyruvate, either alone or in combination, had little effect on MYC protein levels in glutamine-deprived cells (Figs 4C and EV3D). In contrast, addition of a mixture of four ribonucleosides and thymidine largely restored MYC protein expression (Fig 4C). Furthermore, both a mixture of purine nucleosides and adenosine, but neither pyridine nucleosides nor any desoxy-nucleoside, restored expression of MYC in glutamine-deprived cells (Fig 4D). Measurements of nucleotide pools showed that addition of glutamine or adenosine, but not of methylated α -ketoglutarate, reverted the decrease in cellular adenosine-nucleotide levels caused by glutamine deprivation (Fig 4B). Adenosine addition had no significant effect on cellular levels of other ribonucleotides, but led to increased levels of several desoxy-ribonucleotides. Consistent with these observations, a MYC construct that comprises only the coding sequence did not respond to re-addition of adenosine to glutamine-deprived cells, whereas expression of MYC from a construct comprising the 3'-UTR was stimulated by addition of adenosine (Fig EV3E). In line with this, addition of adenosine partially restored translation of MYC in glutamine-deprived cells (Fig 2A). The role of glutamine as donor of amino groups in nucleotide biosynthesis does not require glutaminase; consistently, inhibition of glutaminase by three different inhibitors had no effect on MYC levels (Fig EV4A). We confirmed that two of the inhibitors, BPTES (bis-2-(5-phenylacetamido-1,3,4-thiadiazol-2-yl)ethyl sulfide) and CB839, decreased label incorporation from ^{13}C -glutamine into glutamate and the TCA intermediates α -ketoglutarate and malate (Fig EV4B) and that inhibition of glutaminase had no significant effects on levels of adenosine nucleotides (Fig EV4C). In contrast, steady-state levels of adenosine nucleotides declined within 2 h after glutamine deprivation, paralleling the

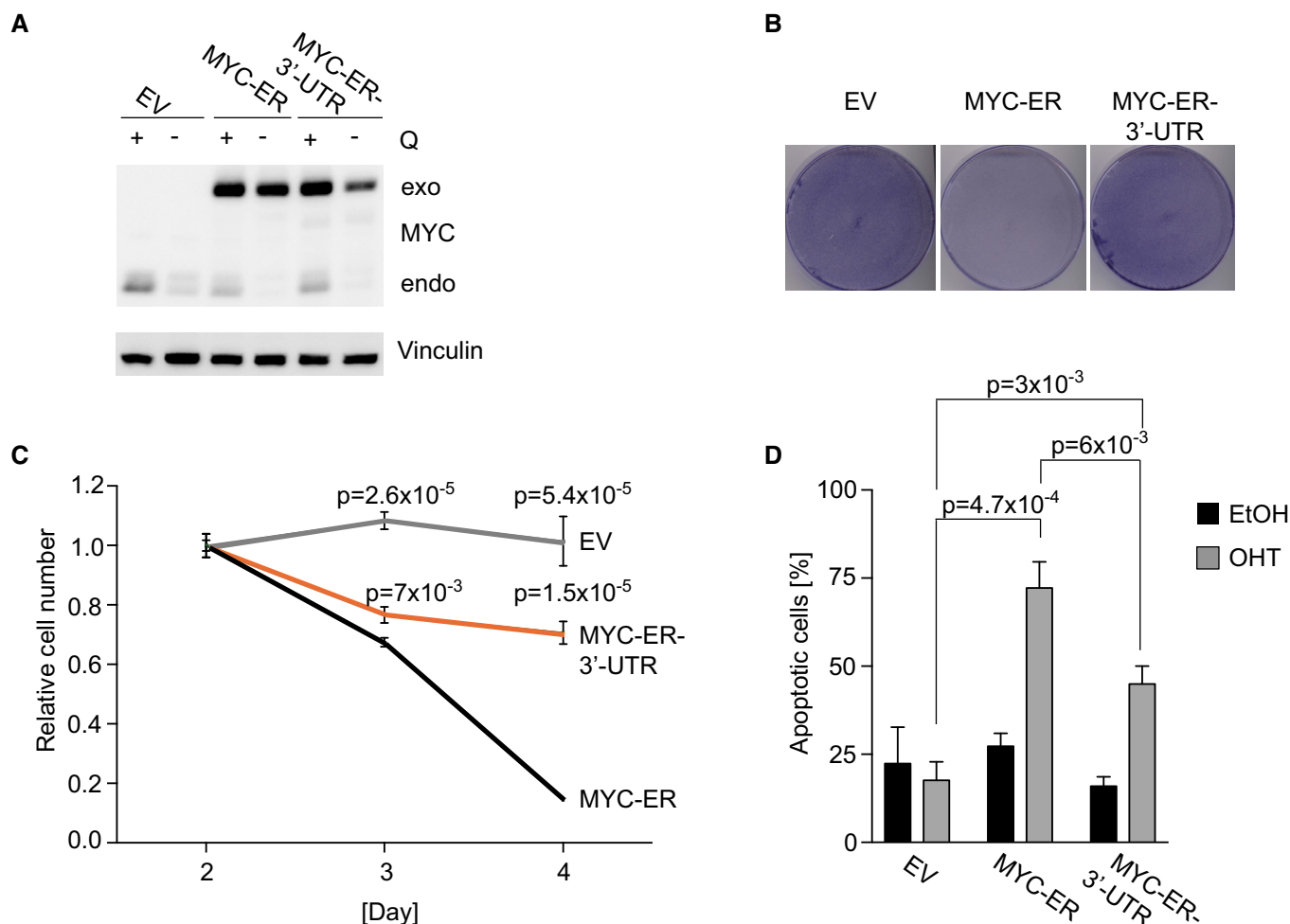


Figure 3. Role of the 3'-UTR in cellular responses to glutamine deprivation.

A Immunoblot of HCT116 cells stably expressing the indicated MYC-ER constructs or empty vector (EV) as control. MYC-ER activity was induced overnight with 20 nM 4-hydroxytamoxifen (OHT), followed by 24 h of glutamine starvation in the presence of OHT ($n = 4$).
B Crystal-violet-stained tissue culture plates documenting growth of HCT116 cells cultured in glutamine-depleted medium for 48 h in the presence of OHT.
C Quantification of relative cell number at the indicated time points after glutamine starvation. Each sample was normalized to the value obtained after 48 h of starvation. Each point represents the mean \pm SD ($n = 3$). P -values were calculated using Student's t -test, comparing EV or MYC-ER-3'-UTR to MYC-ER.
D PI-FACS documenting number of HCT116 cells with a sub-G1 DNA content after 72 h of glutamine starvation. Results show mean \pm SD ($n = 3$). P -values were calculated using Student's t -test.

decrease in MYC levels (Fig 4E). Finally, we found that addition of adenosine to glutamine-deprived cells restored MYC expression, but not cell proliferation, arguing that the increase in MYC is not an indirect consequence of changes in cell proliferation (Fig 4F). We concluded that the MYC 3'-UTR senses cellular adenosine levels to regulate MYC expression.

To understand how glutamine and adenosine levels signal to the 3'-UTR, we profiled expression of microRNAs by RNA sequencing. HCT116 expressed several microRNAs that target the MYC 3'-UTR at significant levels, but glutamine deprivation did not alter expression of any of them (Appendix Table S1). Furthermore, anti-miRNAs targeting 11 of the most strongly expressed miRNAs enhanced MYC protein levels but did not affect regulation of MYC in response to glutamine deprivation (Appendix Fig S3), suggesting that regulation is independent of microRNAs.

Glutamine deprivation has global and MYC-dependent effects on RNAPII function

To understand the physiological relevance of glutamine-dependent regulation of MYC, we initially examined whether activation of MYC in the absence of glutamine depletes critical metabolite pools. However, measurements of multiple metabolite concentrations and reactive oxygen species after 15 h of glutamine deprivation provided no experimental support for this model (Fig EV5A and B). Activation of MYC can have global effects on both promoter binding and elongation by RNA polymerase II (RNAPII) and, in some situations, globally enhances RNAPII function (Rahl *et al*, 2010; Lin *et al*, 2012; Nie *et al*, 2012; Walz *et al*, 2014). To test how regulation of MYC levels by glutamine affects RNAPII function, we measured association of RNAPII with the promoters and of the

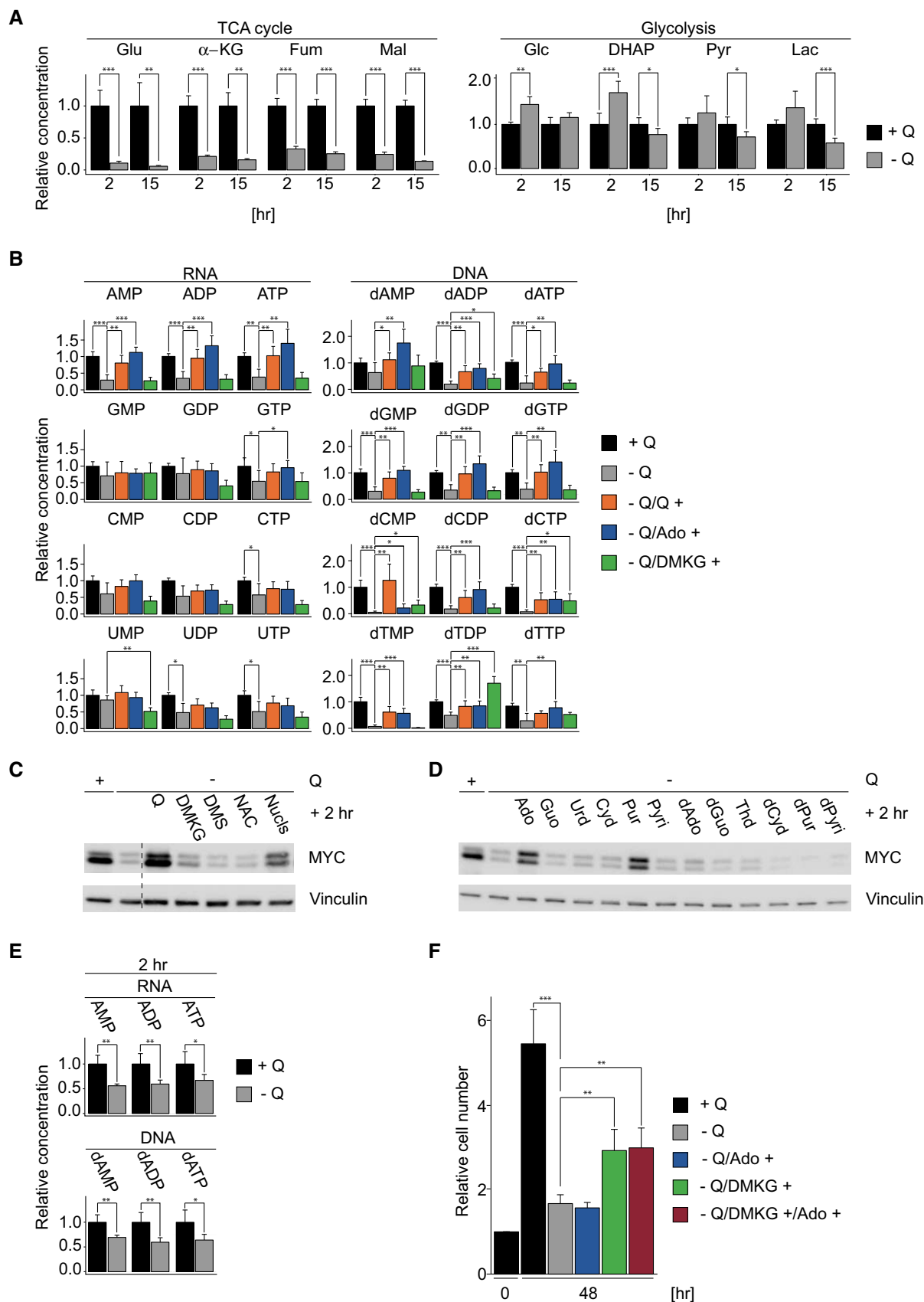


Figure 4.

Figure 4. Glutamine-dependent metabolites affecting MYC expression.

- A Concentrations of selected metabolites after 2 and 15 h of glutamine starvation in HCT116 cells relative to non-starved cells. Glu: glutamate; α -KG: α -ketoglutarate; Fum: fumarate; Mal: malate; DHAP: dihydroxyacetone phosphate; Pyr: pyruvate; Lac: lactate. Data show mean ratios + SD ($n = 6$, each measurement performed in technical duplicates). P -values were calculated using Student's t -test ($***P < 0.001$; $**P < 0.01$; $*P < 0.05$).
- B Concentrations of nucleotides in HCT116 cells that were glutamine-starved for 15 h, followed by re-addition of the indicated substrates for 2 h. DMKG: dimethyl- α -ketoglutarate; Ado: adenosine. Values were normalized to +Q. Data represent mean ratios + SD ($n = 6$, each measurement carried out in triplicates). P -values were calculated using Student's t -test ($***P < 0.001$; $**P < 0.01$; $*P < 0.05$).
- C Immunoblot of glutamine-starved HCT116 cells after addition of the indicated substrates. DMS: dimethyl succinate; NAC: N -acetyl-cysteine; Nucl: mix of five ribo- and deoxy-ribonucleosides ($n = 2$).
- D Immunoblot of glutamine-starved cells after addition of the indicated substrates. Ado: adenosine; Guo: guanosine; Urd: uridine; Cyt: cytidine; Pur: adenosine and guanosine; Pyri: cytidine and uridine; dAdo: deoxy-adenosine; dGuo: deoxy-guanosine; Thd: thymidine; dCyd: deoxy-cytidine; dPur: deoxy-adenosine and deoxy-guanosine; dPyri: thymidine and deoxy-cytidine ($n = 3$).
- E Concentrations of adenosine-derived nucleotides after 2 h of glutamine starvation in HCT116 cells, relative to non-starved cells. Data represent mean ratios + SD ($n = 6$, each measurement carried out in triplicates). P -values were calculated using Student's t -test ($**P < 0.01$; $*P < 0.05$).
- F Numbers of HCT116 cells grown for 48 h in media supplemented with the indicated substrates. Cell numbers were determined at 0 and 48 h and shown relative to 0 h. Results represent mean + SD ($n = 5$, each measurement carried out in duplicates). P -values were calculated using Student's t -test ($***P < 0.001$; $**P < 0.01$).

elongating form of RNAPII, (pSer2 RNAPII) with the transcription end sites (TES) of two highly transcribed genes, *ACTB* (encoding actin B) and *NCL* (encoding nucleolin; Fig 5A; control immunoblots for MYC and RNAPII are shown in Fig EV5C). Both genes showed decreased RNAPII binding to the promoter and association of elongating RNAPII with the TES upon glutamine deprivation. Both effects were largely reverted by activation of MYC-ER. To obtain a global view of RNAPII function, we performed ChIP sequencing under these experimental conditions (Fig EV5C). Inspection of multiple individual traces (Fig 5B) and global analyses (Figs 5C and EV5D) showed that glutamine deprivation globally reduced association of RNAPII with promoters and of elongating RNAPII with the TES. Both decreases were partially reverted upon activation of MYC-ER. Quantitative analyses showed that the decrease in RNAPII binding upon glutamine deprivation and the restoration by MYC were uniform for all promoters where RNAPII binding could be detected (Fig 5D). Similarly, the effect of MYC on Ser2-RNAPII occupancy at the TES was uniform across all active genes (Fig 5D). Addition of adenosine to glutamine-deprived cells restored binding of RNAPII to three promoters that we tested (Fig EV5E), consistent with the effects on MYC levels. In contrast, effects on elongation by RNAPII were variable, most likely due to decreased and varying levels of other ribonucleotides (F. R. Dejure, unpublished observation).

Additional ChIP-sequencing experiments showed that MYC binding was detectable at virtually all promoters transcribed by RNAPII and that—as observed in other cell types—binding of MYC closely paralleled that of RNAPII, arguing that MYC generally occupies active promoters (Fig 5E). Furthermore, the magnitude of the decrease in RNAPII occupancy upon glutamine deprivation and of the restoration by activation of MYC paralleled MYC occupancy (Appendix Fig S4A and B). Previous works had shown that MYC can globally affect both RNAPII binding to promoters and elongation (Rahl *et al*, 2010; Lin *et al*, 2012; Nie *et al*, 2012; Walz *et al*, 2014). The easiest interpretation of these findings is, therefore, that changes in MYC levels directly and globally couple RNAPII function to ribonucleotide and adenosine availability.

Glutamine deprivation alters transcriptional elongation

To ascertain whether RNAPII functions normally in the absence of glutamine, we determined the change in RNAPII association with

promoters versus the change in RNAPII association in the body of the gene for all transcribed genes. Notably, glutamine withdrawal caused a large decrease in RNAPII association with promoters, but a smaller decrease in RNAPII association with gene bodies (Fig 6A). Consistently, glutamine starvation led to a decrease in the traveling ratio of RNAPII, which is the ratio of RNAPII bound at promoters relative to RNAPII bound in gene bodies, suggesting that glutamine withdrawal decreases pause-release or slows down transcriptional elongation (Fig 6B).

Activation of MYC-ER in the absence of glutamine partially reverted the decrease in the traveling ratio, consistent with multiple previous observations that MYC promotes pause-release and elongation and transfers elongation factors onto RNAPII (Fig 6B; Rahl *et al*, 2010; Jaenicke *et al*, 2016). However, the effect of MYC was not uniform for all genes: RNAPII association with the gene body increased on 176 genes upon MYC activation in the absence of glutamine to levels higher than in control cells grown in the presence of glutamine although levels of RNAPII at the promoter remained lower than in glutamine-replete cells, suggesting that activation of MYC in the absence of glutamine promotes stalling of RNAPII on these genes. The strongest accumulation of RNAPII in the gene body was observed in the *TKT* gene, which encodes transketolase, an enzyme of the pentose phosphate pathway (Fig 6C and D).

Defects in elongation prolong both the proximity of nascent RNA with RNAPII and transcription-dependent supercoiling of DNA, and both factors promote the formation of R-loops (Costantino & Koshland, 2015). To test whether stalling of RNAPII correlates with R-loop formation, we immunoprecipitated chromatin using a monoclonal antibody (S9.6) that recognizes RNA/DNA hybrids and—as control—treated an aliquot of the immunoprecipitates with RNaseH1 (Skourti-Stathaki *et al*, 2011). We selected multiple primers that cover the *TKT* gene on which stalling was observed upon MYC activation (Fig 6D). This analysis showed that the region in which stalling was observed had a high propensity for R-loop formation (Fig 6E). To determine the effect of glutamine starvation and MYC activation, we measured R-loop accumulation in glutamine-containing medium and in cells depleted of glutamine, both with and without activation of MYC-ER. In these experiments, activation of MYC-ER caused a significant accumulation of R-loops in glutamine-starved cells (Fig 6F). Taken together, our data show that activation of MYC-ER in glutamine-deprived cells leads to stalling of RNAPII and R-loop formation.

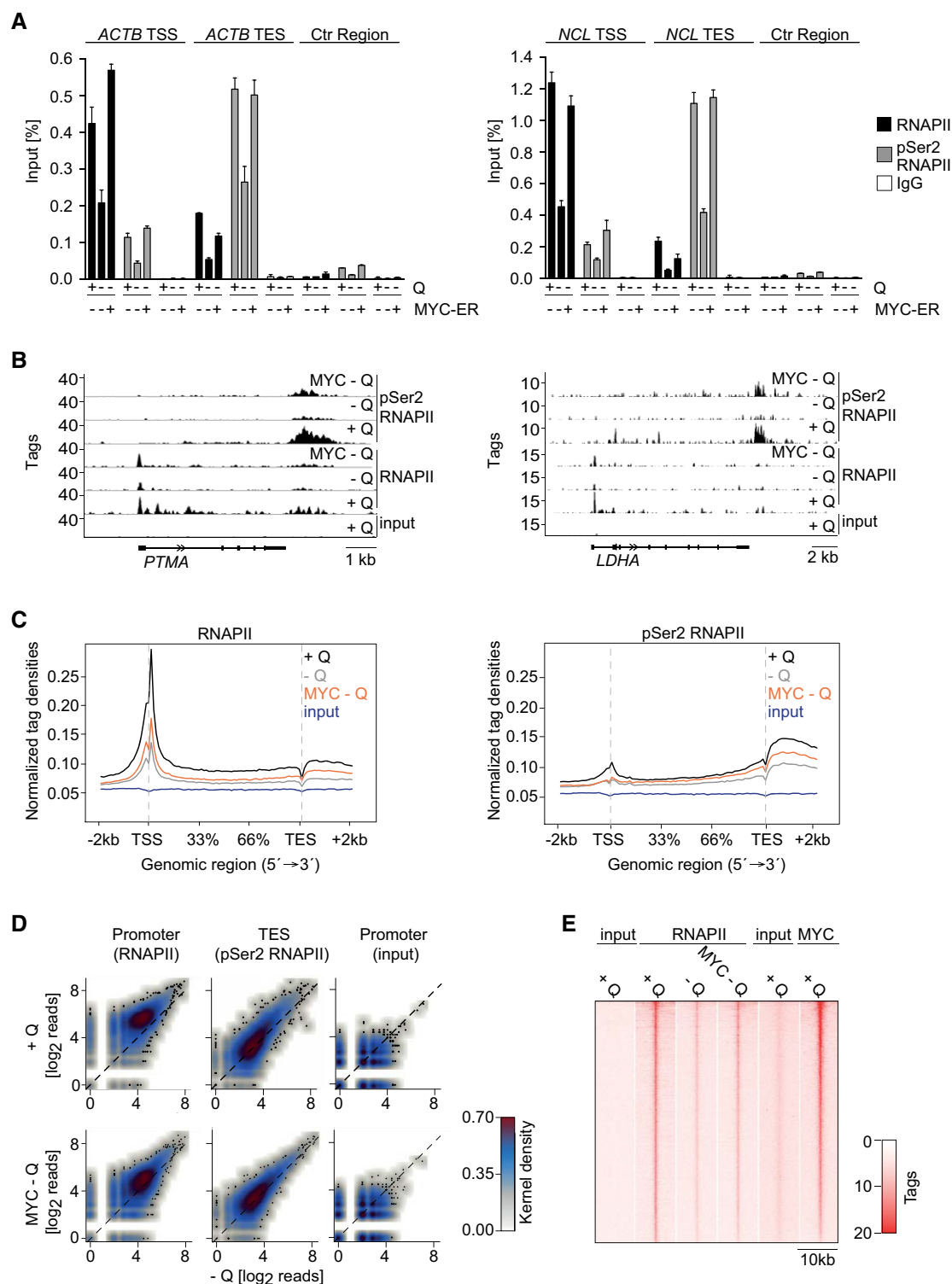


Figure 5. Effects of glutamine starvation on RNAPII function.

- A ChIP experiment documenting RNAPII binding to the transcription start site (TSS) and transcription end site (TES) of the *ACTB* and *NCL* genes and an intergenic control region (same for both targets). MYC-ER activity was induced overnight with 100 nM OHT. Cells were starved for 5 h in the presence of OHT. Bars represent mean + SD of technical triplicates.
- B ChIP-sequencing tracks for *PTMA* and *LDHA* from HCT116 cells treated as in panel (A).
- C Metagenome plots of RNAPII (left) or pSer2 RNAPII (right) for all genes with detectable RNAPII binding under the indicated conditions.
- D Density plots comparing occupancy by RNAPII at the TSS and by pSer2 RNAPII at the TES for all genes with detectable RNAPII binding under the indicated conditions.
- E Heat map showing promoter occupancy by RNAPII and by MYC for all promoters ($n = 9,796$) at which RNAPII binding is detectable.

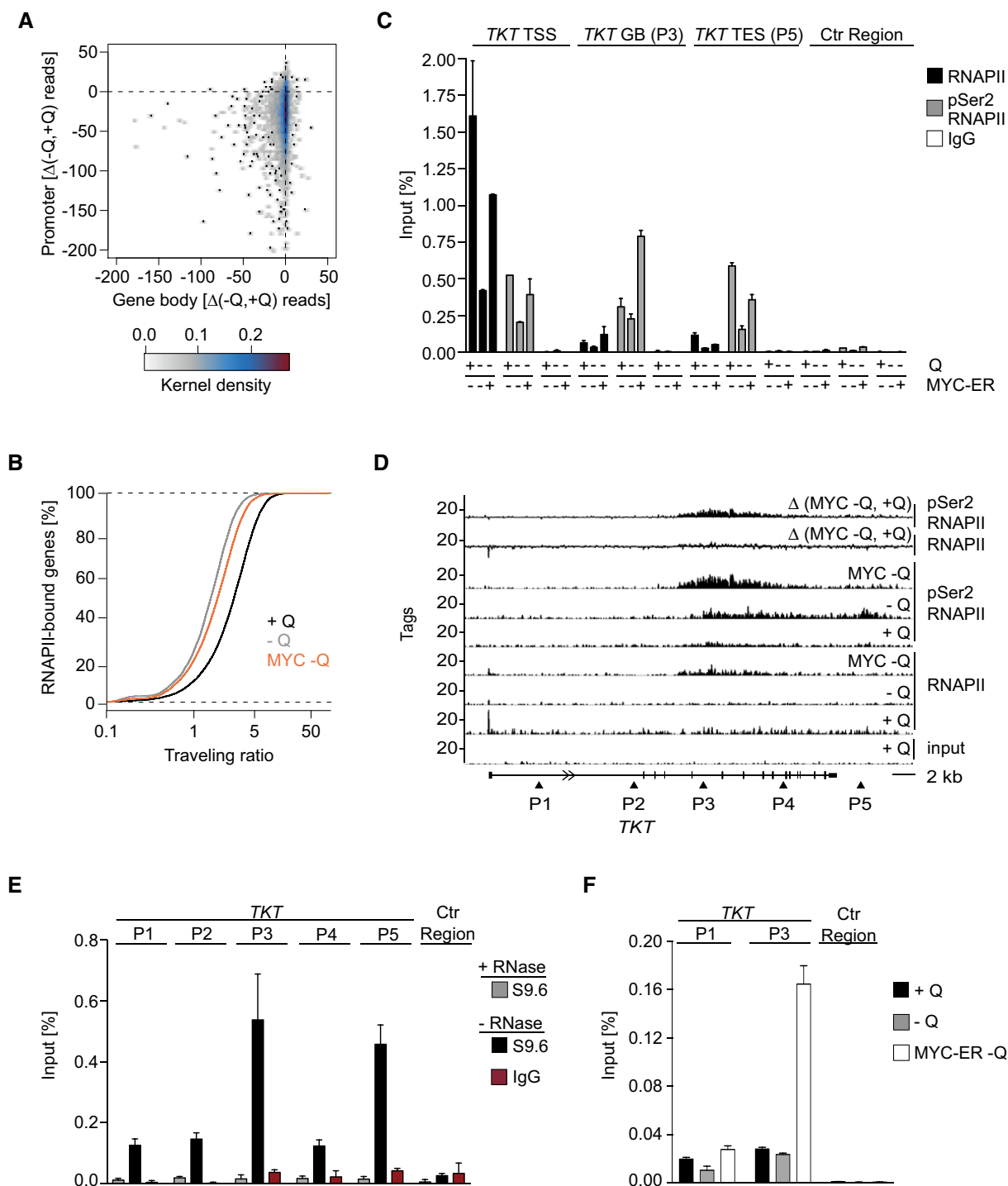


Figure 6. Analysis of transcriptional elongation by RNAPII and R-loop formation.

A Kernel density plot documenting the effect of glutamine starvation on RNAPII occupancy at the promoter and in the gene body for all genes with detectable RNAPII binding (Δ : difference between the indicated conditions). Outliers are shown as black dots.

B Traveling ratio of RNAPII under the indicated experimental conditions.

C ChIP-sequencing track showing MYC-ER-mediated RNAPII accumulation in the gene body (GB) of *TKT*. See panel (D) for position of primers.

D ChIP experiment documenting RNAPII occupancy at the TSS, an intragenic site, and the TES of the *TKT* gene upon MYC-ER activation. Description as in Fig 5A. Bars represent mean \pm SD of technical triplicates ($n = 2$).

E DNA-RNA immunoprecipitation (DIP) showing the presence of R-loops in the *TKT* gene. HCT116 cells were starved for 5 h. DNA was extracted, treated or not with RNase, and immunoprecipitated with S9.6 antibody or IgG as control. Bars represent mean \pm SD of technical triplicates.

F DIP assays showing R-loops under the indicated experimental conditions. MYC-ER- or EV-expressing cells were induced overnight with 100 nM OHT and then starved for 24 h in the presence of OHT. Bars represent mean \pm SD of technical triplicates ($n = 2$).

Discussion

A large body of work has shown that expression of the *MYC* mRNA is responsive to external growth factors and to growth inhibitory factors such as TGF- β (Meyer & Penn, 2008). Similarly, recent work has documented that several stress-responsive pathways and individual miRNAs have the potential to suppress *MYC* expression (see Introduction). The physiological significance of the latter regulation has not yet been firmly established. We show here, using the paradigm of glutamine starvation, that the 3'-UTR couples *MYC* translation to the cellular metabolic status and specifically to the availability of adenosine nucleotides, which are the ribonucleotides that most strongly depend on glutamine. The *MYC* 3'-UTR is not mutated in human tumors, suggesting that this regulatory mechanism is intact in tumor cells. This conclusion is supported by the analysis of several colon tumor cell lines. A plethora of miRNAs and RNA-binding proteins bind to and regulate *MYC* via the 3'-UTR. We did not obtain evidence for involvement of microRNAs in glutamine-dependent *MYC* translation; hence, the detailed mechanism by which glutamine levels signal to the *MYC* 3'-UTR remains to be determined. However, many nucleotide-binding enzymes are known to moonlight as RNA-interacting proteins (Castello *et al*, 2012, 2015). It is therefore tempting to speculate that a decrease in adenosine-nucleotide levels changes the *MYC* mRNA interactome to regulate *MYC* translation.

MYC binds to essentially all open promoters in tumor cells (Sabo *et al*, 2014; Walz *et al*, 2014) and changes in *MYC* levels can globally enhance association of RNAPII with promoters (Walz *et al*, 2014) as well as pause-release and elongation (Rahl *et al*, 2010; Walz *et al*, 2014; Jaenicke *et al*, 2016). These findings raise the possibility that glutamine regulation of *MYC* levels serves to globally couple RNAPII function to the availability of nucleotides. Consistent with this notion, glutamine deprivation elicited a global decrease in RNAPII promoter association and elongation at virtually all genes that we analyzed. Under these conditions, nucleotide levels decrease rapidly; hence, changes in RNAPII function might be secondary to altered ribonucleotide levels. Concentrations of ribonucleotide triphosphates in tumor cells are estimated to be between 400 μ M (CTP) and 3,000 μ M (ATP) (Traut, 1994) and thus significantly exceed the K_M values of RNAPII for transcriptional initiation (around 10 μ M for ATP; Jiang & Gralla, 1995). We therefore consider it unlikely that the magnitude of the decrease in ribonucleotide triphosphate levels observed after glutamine deprivation has a significant direct impact on promoter association by RNAPII. Instead, we show that activation of *MYC*-ER restores RNAPII binding to promoters to a large degree. The simplest explanation of our observations is therefore that the low *MYC* levels in glutamine-starved cells limit RNAPII function, consistent with the notion that *MYC* levels can be rate-limiting for transcription (Lin *et al*, 2012; Nie *et al*, 2012).

In glutamine-deprived cells, RNAPII binding to promoter decreases strongly, but the decrease in RNAPII association with the gene body is more moderate, resulting in a decreased traveling ratio of RNAPII. During elongation, RNAPII oscillates between forward and backward movements in response to nucleotide misincorporation and overall elongation speed hence depends on absolute and relative nucleotide concentrations (Toulme *et al*, 1999). The decrease in traveling ratio indicates a reduced pause-release or

reduced elongation rate and possibly stalling of RNAPII. Activation of *MYC* in glutamine-deprived cells partially reverts the global decrease in traveling ratio, but has no effect on ribonucleotide levels. Importantly, restoration of elongation by *MYC* is not perfect: Rather there is a significant increase in RNAPII stalling on approximately 200 genes. The strongest increase is observed on the *TKT* gene in a sequence that can form an R-loop. R-loops contain single-stranded DNA, which is prone to base modifications and mutagenesis (Costantino & Koshland, 2015). Notably, glutamine deprivation also causes accumulation of reactive oxygen species, which are a significant cause of DNA damage at single-stranded DNA. Finally, R-loops, if unresolved, can cause replication/transcription conflicts arguing that even individual R-loops can be a major source of DNA damage and genomic instability (Helmrich *et al*, 2013). Both replication stress and overt DNA damage contribute to induction of apoptosis by deregulated *MYC* (Reimann *et al*, 2007; Murga *et al*, 2011). We propose, therefore, that regulation of RNAPII function by glutamine via *MYC* protects cells from the deleterious consequences of global transcriptional elongation when nucleotide concentrations are low. Intriguingly, the identification of a consistent group of downstream target genes and pathways, by which *MYC* induces apoptosis, has remained difficult. Our data suggest an alternative model, in which the global stimulation of transcription elongation by deregulated *MYC* induces apoptosis since it generates aberrant transcription structures, such as R-loops, in metabolically stressed cells (Fig 7). It remains to be determined whether this model can generally account for *MYC*-dependent apoptosis during tumorigenesis.

Exploiting glutamine addiction is a paradigm example of therapeutic strategies that rely on the pro-apoptotic properties of deregulated *MYC*. Our data have two implications for these strategies: First, current approaches rely on inhibition of glutaminase and our data show that several glutaminase inhibitors have no effect on adenosine and *MYC* levels in colon cancers cells, arguing that targeting nucleotide synthesis may target *MYC*-driven tumors more directly. Second, tumorigenesis in *MYC*-driven transgenic mouse models is limited by *MYC*-dependent apoptosis and greatly accelerated by inhibition of apoptosis provided by ectopic expression of Bcl2 family members of loss of the Arf and p53 tumor suppressor (Eischen *et al*, 1999; Finch *et al*, 2006; Wang *et al*, 2011), but whether deregulated *MYC* expression establishes a dependence on specific anti-apoptotic mechanisms in human tumors is less clear. We show here that the 3'-UTR enables colon tumor cells with deregulated *MYC* expression to escape from apoptosis upon metabolic stress, since it ensures that *MYC* protein expression remains stress-responsive even though the promoter is constitutively active. Many currently used *MYC* transgenes, including those used to characterize pro-apoptotic properties of deregulated *MYC* *in vivo* (Felsher & Bishop, 1999; Murphy *et al*, 2008; Wang *et al*, 2011), lack the 3'-UTR. Since tumors frequently grow in hypoxic and nutrient-deprived environments (Stine *et al*, 2015), such transgenes may overestimate *MYC*'s pro-apoptotic potential. Conversely, translation of endogenous *MYC* is driven from an internal ribosome entry site (IRES) in the 5'-UTR during staurosporine- and TRAIL-induced apoptosis (Stoneley *et al*, 2000), arguing that IRES-driven translation of *MYC* may not be subject to repression by the 3'-UTR. We propose, therefore, that therapeutic strategies that aim to exploit *MYC*'s pro-apoptotic potential for tumor therapy need to inhibit or bypass the pathways that suppress *MYC* expression *in vivo* to be successful.

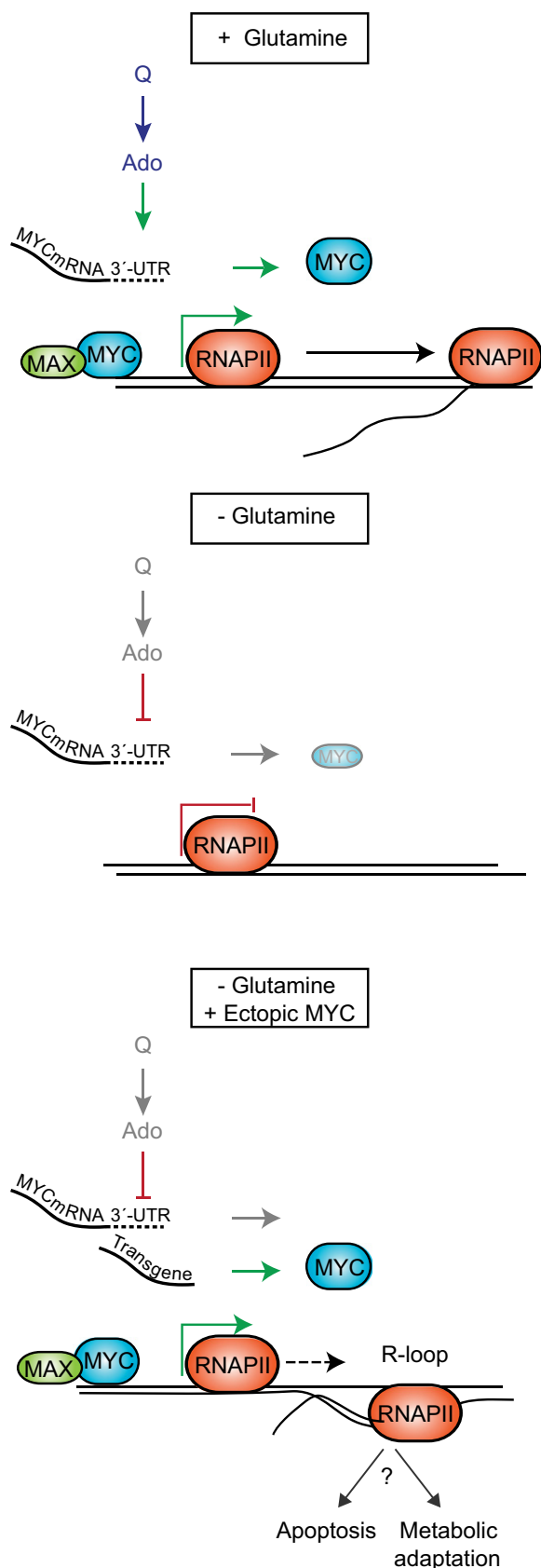


Figure 7. Model summarizing our findings

Finally, we note that transketolase, the enzyme encoded by the *TKT* gene, in which RNAPII stalling is particularly strong and correlates with R-loop formation, itself has a critical role in nucleotide biosynthesis, since TKT levels influence whether glucose that enters the pentose phosphate pathway is used for synthesis of nucleotides or for synthesis of reducing equivalents to counteract oxidative stress (Xu *et al*, 2016). R-loops also have signaling functions independent from causing DNA damage (Tresini *et al*, 2015). It is possible, therefore, that RNAPII stalling and R-loop formation also control metabolic enzyme levels or serve as a sensor during the metabolic adaptation to glutamine starvation (Fig 7).

Materials and Methods

Cell culture and reagents

All reagents were purchased from Sigma, unless otherwise indicated. All cell lines were obtained from ATCC. Cell lines were maintained in DMEM supplemented with 10% FBS (Biocrom) and 1% penicillin/streptomycin and validated using STR analysis. Cell lines were routinely tested for mycoplasma contamination. Experiments were performed using DMEM reconstituted with 2 mM glutamine, 2.5 g/l glucose, 0.015 g/l phenol red, 10% dialyzed FBS, and 1% penicillin/streptomycin, without sodium pyruvate, unless specific concentrations are indicated. For starvation experiments, cells were washed twice with PBS and cultured in reconstituted DMEM without glucose or glutamine. For single amino acids starvation (Q; M; L) medium lacking each amino acid was prepared in Earle's balanced salt solution supplemented with MEM vitamin solution (Life Technologies), 2.5 g/l glucose, 10% dialyzed FBS, 0.0001 g/l $\text{Fe}(\text{NO}_3)_3 \cdot 9\text{H}_2\text{O}$, and the remaining amino acids according to the DMEM composition. Where specified, the following reagents were added at the indicated final concentrations: ^{13}C -glutamine (Cambridge Isotopes Laboratories Inc., 2 mM), dimethyl- α -KG (7 mM), dimethyl succinate (20 mM), sodium pyruvate (1 mM), *N*-acetyl cysteine (5 mM), glutathione-reduced ethyl ester (5 mM), nucleoside mix (Merck Millipore, 5 \times), glutamate (1.35 mM), nucleosides and deoxynucleosides (150 μM , except for thymidine, used at 50 μM), cycloheximide (100 $\mu\text{g}/\text{ml}$, dissolved in EtOH), MG132 (Calbiochem/Millipore, 20 μM , dissolved in DMSO), 4-hydroxytamoxifen (100 nM, dissolved in EtOH), doxycycline (1 $\mu\text{g}/\text{ml}$, dissolved in EtOH). Rapamycin (LC Laboratories, 20 nM), OSI-027 (Active Biochemicals, 20 μM), CB-839 (Selleckchem, 10 μM), BPTES, and Compound 968 (Calbiochem/Millipore, 10 μM) were all dissolved in DMSO.

ChIP, ChIP sequencing, and DIP

ChIP experiments were performed as described previously (Walz *et al*, 2014). The DIP experiment was adapted from a published protocol (Weber *et al*, 2005). Cells were harvested, digested overnight in a buffer containing SDS and proteinase K, and sonified to random fragments with a size between 100 and 200 bp. Genomic DNA was purified by phenol-chloroform extraction and either treated with 20 U of RNaseH (NEB) overnight or not. Immunoprecipitation was performed using monoclonal antibody S9.6 and protein G- and protein A-coupled Dynabeads without final de-cross-linking. Sequencing was performed using NextSeq 500 Illumina platform.

GC-MS and direct infusion MS analysis

Metabolite extraction was carried out as described in Kempa *et al* (2009). Nucleotides were extracted as described in Lorkiewicz *et al* (2012). See Appendix Supplementary Methods for detailed protocols.

Statistical analyses

Statistical analysis was performed using Prism software (GraphPad), and R. Statistical significance was tested with heteroscedastic two-tailed Student's *t*-tests. Data are presented as mean, and error bars show standard deviation of the indicated number of biological replicates.

Data availability

ChIP-sequencing datasets are available at the Gene Expression Omnibus under the accession number GEO: GSE86556.

Expanded View for this article is available online.

Acknowledgements

We thank Dr. Chris Bielow for providing R-scripts for analysis of metabolomics data and Stephen Leppla (NIH) for the S9.6 antibody. This work was funded by grants from the German Research Council to M.E. (DFG 222/12-1), to F.R.D. via the Graduate School of Life Sciences, to N.R. via the Berlin School of Integrative Oncology, and to E.W. via (WO 2108/1-1).

Author contributions

FRD, NR, CPA, GM, JK, EW, and JTV performed the experiments, SW analyzed high-throughput data, SH, AS, SK, and ME devised and supervised experiments, and SK and ME wrote the manuscript.

Conflict of interest

The authors declare that they have no conflict of interest.

References

- Annibali D, Whitfield JR, Favuzzi E, Jauset T, Serrano E, Cuartas I, Redondo-Campos S, Folch G, Gonzalez-Junca A, Sodir NM, Masso-Valles D, Beaulieu ME, Swigart LB, Mc Gee MM, Somma MP, Nasi S, Seoane J, Evan GI, Soucek L (2014) Myc inhibition is effective against glioma and reveals a role for Myc in proficient mitosis. *Nat Commun* 5: 4632
- Barna M, Pusic A, Zollo O, Costa M, Kondrashov N, Rego E, Rao PH, Ruggero D (2008) Suppression of Myc oncogenic activity by ribosomal protein haploinsufficiency. *Nature* 456: 971–975
- Bhagwat SV, Gokhale PC, Crew AP, Cooke A, Yao Y, Mantis C, Kahler J, Workman J, Bittner M, Dudkin L, Epstein DM, Gibson NW, Wild R, Arnold LD, Houghton PJ, Pachter JA (2011) Preclinical characterization of OSI-027, a potent and selective inhibitor of mTORC1 and mTORC2: distinct from rapamycin. *Mol Cancer Ther* 10: 1394–1406
- Bott AJ, Peng IC, Fan Y, Faubert B, Zhao L, Li J, Neidler S, Sun Y, Jaber N, Krokowski D, Lu W, Pan JA, Powers S, Rabinowitz J, Hatzoglou M, Murphy DJ, Jones R, Wu S, Girmun G, Zong WX (2015) Oncogenic Myc induces expression of glutamine synthetase through promoter demethylation. *Cell Metab* 22: 1068–1077
- Cannell IG, Kong YW, Johnston SJ, Chen ML, Collins HM, Dobbyn HC, Elia A, Kress TR, Dickens M, Clemens MJ, Heery DM, Gaestel M, Eilers M, Willis AE, Bushell M (2010) p38 MAPK/MK2-mediated induction of miR-34c following DNA damage prevents Myc-dependent DNA replication. *Proc Natl Acad Sci USA* 107: 5375–5380
- Carroll PA, Diolaiti D, McFerrin L, Gu H, Djukovic D, Du J, Cheng PF, Anderson S, Ulrich M, Hurley JB, Raftery D, Ayer DE, Eisenman RN (2015) Deregulated Myc requires MondoA/Mlx for metabolic reprogramming and tumorigenesis. *Cancer Cell* 27: 271–285
- Castello A, Fischer B, Eichelbaum K, Horos R, Beckmann BM, Strein C, Davey NE, Humphreys DT, Preiss T, Steinmetz LM, Krijgsvelde J, Hentze MW (2012) Insights into RNA biology from an atlas of mammalian mRNA-binding proteins. *Cell* 149: 1393–1406
- Castello A, Hentze MW, Preiss T (2015) Metabolic enzymes enjoying new partnerships as RNA-binding proteins. *Trends Endocrinol Metab* 26: 746–757
- Christoffersen NR, Shalgi R, Frankel LB, Leucci E, Lees M, Klausen M, Pilpel Y, Nielsen FC, Oren M, Lund AH (2010) p53-independent upregulation of miR-34a during oncogene-induced senescence represses MYC. *Cell Death Differ* 17: 236–245
- Costantino L, Koshland D (2015) The Yin and Yang of R-loop biology. *Curr Opin Cell Biol* 34: 39–45
- Dang CV (2011) Therapeutic targeting of Myc-reprogrammed cancer cell metabolism. *Cold Spring Harb Symp Quant Biol* 76: 369–374
- Dang CV (2012) MYC on the path to cancer. *Cell* 149: 22–35
- Doherty JR, Yang C, Scott KE, Cameron MD, Fallahi M, Li W, Hall MA, Amelio AL, Mishra JK, Li F, Tortosa M, Genau HM, Rounbehler RJ, Lu Y, Dang CV, Kumar KG, Butler AA, Bannister TD, Hooper AT, Unsal-Kacmaz K *et al* (2014) Blocking lactate export by inhibiting the Myc target MCT1 Disables glycolysis and glutathione synthesis. *Can Res* 74: 908–920
- Duran RV, Oppliger W, Robitaille AM, Heiserich L, Skendaj R, Gottlieb E, Hall MN (2012) Glutaminolysis activates Rag-mTORC1 signaling. *Mol Cell* 47: 349–358
- Eberhardy SR, Farnham PJ (2001) c-Myc mediates activation of the cad promoter via a post-RNA polymerase II recruitment mechanism. *J Biol Chem* 276: 48562–48571
- Eischen CM, Weber JD, Roussel MF, Sherr CJ, Cleveland JL (1999) Disruption of the ARF-Mdm2-p53 tumor suppressor pathway in Myc-induced lymphomagenesis. *Genes Dev* 13: 2658–2669
- Felig P, Marliss E, Ohman JL, Cahill CF Jr (1970) Plasma amino acid levels in diabetic ketoacidosis. *Diabetes* 19: 727–728
- Felsher DW, Bishop JM (1999) Reversible tumorigenesis by MYC in hematopoietic lineages. *Mol Cell* 4: 199–207
- Finch A, Prescott J, Shchors K, Hunt A, Soucek L, Dansen TB, Swigart LB, Evan GI (2006) Bcl-xL gain of function and p19 ARF loss of function cooperate oncogenically with Myc *in vivo* by distinct mechanisms. *Cancer Cell* 10: 113–120
- Gao P, Tchernyshyov I, Chang TC, Lee YS, Kita K, Ochi T, Zeller KI, De Marzo AM, Van Eyk JE, Mendell JT, Dang CV (2009) c-Myc suppression of miR-23a/b enhances mitochondrial glutaminase expression and glutamine metabolism. *Nature* 458: 762–765
- Gouw AM, Toal GG, Felsher DW (2016) Metabolic vulnerabilities of MYC-induced cancer. *Oncotarget* 21: 29879–29880
- Hann SR, King MW, Bentley DL, Anderson CW, Eisenman RN (1988) A non-AUG translational initiation in c-myc exon 1 generates an N-terminally distinct protein whose synthesis is disrupted in Burkitt's lymphomas. *Cell* 52: 185–195
- He TC, Sparks AB, Rago C, Hermeking H, Zawel L, da Costa LT, Morin PJ, Vogelstein B, Kinzler KW (1998) Identification of c-MYC as a target of the APC pathway. *Science* 281: 1509–1512
- He L, He X, Lim LP, de Stanchina E, Xuan Z, Liang Y, Xue W, Zender L, Magnus J, Ridzon D, Jackson AL, Linsley PS, Chen C, Lowe SW, Cleary MA,

- Hannon GJ (2007) A microRNA component of the p53 tumour suppressor network. *Nature* 447: 1130–1134
- Helmrich A, Ballarino M, Nudler E, Tora L (2013) Transcription-replication encounters, consequences and genomic instability. *Nat Struct Mol Biol* 20: 412–418
- Hermeking H (2007) p53 enters the microRNA world. *Cancer Cell* 12: 414–418
- Hsu PP, Sabatini DM (2008) Cancer cell metabolism: Warburg and beyond. *Cell* 134: 703–707
- Jaenicke LA, von Eyss B, Carstensen A, Wolf E, Xu W, Greifenberg AK, Geyer M, Eilers M, Popov N (2016) Ubiquitin-dependent turnover of MYC antagonizes MYC/PAF1C complex accumulation to drive transcriptional elongation. *Mol Cell* 61: 54–67
- Jiang Y, Gralla JD (1995) Nucleotide requirements for activated RNA polymerase II open complex formation *in vitro*. *J Biol Chem* 270: 1277–1281
- Kempa S, Hummel J, Schwemmer T, Pietzke M, Strehmel N, Wienkoop S, Kopka J, Weckwerth W (2009) An automated GCxGC-TOF-MS protocol for batch-wise extraction and alignment of mass isotopomer matrixes from differential 13C-labelling experiments: a case study for photoautotrophic-mixotrophic grown *Chlamydomonas reinhardtii* cells. *J Basic Microbiol* 49: 82–91
- Kim HH, Kuwano Y, Srikantan S, Lee EK, Martindale JL, Gorospe M (2009) HuR recruits let-7/RISC to repress c-Myc expression. *Genes Dev* 23: 1743–1748
- Kress TR, Cannell IG, Brenkman AB, Samans B, Gaestel M, Roepman P, Burgering BM, Bushell M, Rosenwald A, Eilers M (2011) The MK5/PRAK kinase and Myc form a negative feedback loop that is disrupted during colorectal tumorigenesis. *Mol Cell* 41: 445–457
- Kress TR, Sabo A, Amati B (2015) MYC: connecting selective transcriptional control to global RNA production. *Nat Rev Cancer* 15: 593–607
- Lal A, Navarro F, Maher CA, Maliszewski LE, Yan N, O'Day E, Chowdhury D, Dykxhoorn DM, Tsai P, Hofmann O, Becker KG, Gorospe M, Hide W, Lieberman J (2009) miR-24 Inhibits cell proliferation by targeting E2F2, MYC, and other cell-cycle genes via binding to "seedless" 3'UTR microRNA recognition elements. *Mol Cell* 35: 610–625
- Lin CY, Loven J, Rahl PB, Paranal RM, Burge CB, Bradner JE, Lee TI, Young RA (2012) Transcriptional amplification in tumor cells with elevated c-Myc. *Cell* 151: 56–67
- Lorenzin F, Benary U, Jung LA, von Eyß B, Walz S, Kisker C, Wolf J, Eilers M, Wolf E (2016) Promoter affinity is a critical determinant of the specific gene expression patterns elicited by different MYC levels. *eLife* 5: e15161
- Lorkiewicz P, Higashi RM, Lane AN, Fan TW (2012) High information throughput analysis of nucleotides and their isotopically enriched isotopologues by direct-infusion FTICR-MS. *Metabolomics* 8: 930–939
- Meyer N, Penn LZ (2008) Reflecting on 25 years with MYC. *Nat Rev Cancer* 8: 976–990
- Mihailovich M, Bremang M, Spadotto V, Musiani D, Vitale E, Varano G, Zambelli F, Mancuso FM, Cairns DA, Pavesi G, Casola S, Bonaldi T (2015) miR-197-92 fine-tunes MYC expression and function to ensure optimal B cell lymphoma growth. *Nat Commun* 6: 8725
- Murga M, Campaner S, Lopez-Contreras AJ, Toledo LI, Soria R, Montaña MF, D'Artista L, Schleker T, Guerra C, Garcia E, Barbacid M, Hidalgo M, Amati B, Fernandez-Capetillo O (2011) Exploiting oncogene-induced replicative stress for the selective killing of Myc-driven tumors. *Nat Struct Mol Biol* 18: 1331–1335
- Murphy DJ, Junttila MR, Pouyet L, Karnezis A, Shchors K, Bui DA, Brown-Swigart L, Johnson L, Evan GI (2008) Distinct thresholds govern Myc's biological output *in vivo*. *Cancer Cell* 14: 447–457
- Nicklin P, Bergman P, Zhang B, Triantafellow E, Wang H, Nyfeler B, Yang H, Hild M, Kung C, Wilson C, Myer VE, MacKeigan JP, Porter JA, Wang YK, Cantley LC, Finan PM, Murphy LO (2009) Bidirectional transport of amino acids regulates mTOR and autophagy. *Cell* 136: 521–534
- Nie Z, Hu G, Wei G, Cui K, Yamane A, Resch W, Wang R, Green DR, Tessarollo L, Casellas R, Zhao K, Levens D (2012) c-Myc is a universal amplifier of expressed genes in lymphocytes and embryonic stem cells. *Cell* 151: 68–79
- Penn LJZ, Brooks MW, Laufer EM, Land H (1990) Negative autoregulation of c-myc transcription. *EMBO J* 9: 113–121
- Polakis P (1999) The oncogenic activation of beta-catenin. *Curr Opin Genet Dev* 9: 15–21
- Qing G, Li B, Vu A, Skuli N, Walton ZE, Liu X, Mayes PA, Wise DR, Thompson CB, Maris JM, Hogarty MD, Simon MC (2012) ATF4 regulates MYC-mediated neuroblastoma cell death upon glutamine deprivation. *Cancer Cell* 22: 631–644
- Rahl PB, Lin CY, Seila AC, Flynn RA, McQuine S, Burge CB, Sharp PA, Young RA (2010) c-Myc regulates transcriptional pause release. *Cell* 141: 432–445
- Reimann M, Lodenkemper C, Rudolph C, Schildhauer I, Teichmann B, Stein H, Schlegelberger B, Dorken B, Schmitt CA (2007) The Myc-evoked DNA damage response accounts for treatment resistance in primary lymphomas *in vivo*. *Blood* 110: 2996–3004
- Sabo A, Kress TR, Pelizzola M, de Pretis S, Gorski MM, Tesi A, Morelli MJ, Bora P, Doni M, Verrecchia A, Tonelli C, Fagà G, Bianchi V, Ronchi A, Low D, Müller H, Guccione E, Campaner S, Amati B (2014) Selective transcriptional regulation by Myc in cellular growth control and lymphomagenesis. *Nature* 511: 488–492
- Sansom OJ, Meniel VS, Muncan V, Phesse TJ, Wilkins JA, Reed KR, Vass JK, Athineos D, Clevers H, Clarke AR (2007) Myc deletion rescues Apc deficiency in the small intestine. *Nature* 446: 676–679
- Sears R, Nuckolls F, Haura E, Taya Y, Tamai K, Nevins JR (2000) Multiple Ras-dependent phosphorylation pathways regulate Myc protein stability. *Genes Dev* 14: 2501–2514
- Shim H, Dolde C, Lewis BC, Wu CS, Dang C, Jungmann RA, Dalla-Favera R, Dang CV (1997) c-Myc transactivation of LDH-A: implications for tumor metabolism and growth. *Proc Natl Acad Sci USA* 94: 6658–6663
- Skourti-Stathaki K, Proudfoot NJ, Gromak N (2011) Human senataxin resolves RNA/DNA hybrids formed at transcriptional pause sites to promote Xrn2-dependent termination. *Mol Cell* 42: 794–805
- Soucek L, Whitfield J, Martins CP, Finch AJ, Murphy DJ, Sodir NM, Karnezis AN, Swigart LB, Nasi S, Evan GI (2008) Modelling Myc inhibition as a cancer therapy. *Nature* 455: 679–683
- Stine ZE, Walton ZE, Altman BJ, Hsieh AL, Dang CV (2015) MYC, metabolism, and cancer. *Cancer Discov* 5: 1024–1039
- Stoneley M, Chappell SA, Jopling CL, Dickens M, MacFarlane M, Willis AE (2000) c-Myc protein synthesis is initiated from the internal ribosome entry segment during apoptosis. *Mol Cell Biol* 20: 1162–1169
- Toulme F, Guerin M, Robichon N, Leng M, Rahmouni AR (1999) *In vivo* evidence for back and forth oscillations of the transcription elongation complex. *EMBO J* 18: 5052–5060
- Traut TW (1994) Physiological concentrations of purines and pyrimidines. *Mol Cell Biochem* 140: 1–22
- Tresini M, Warmerdam DO, Kolovos P, Snijder L, Vrouwe MG, Demmers JA, van Ijcken WF, Grosveld FG, Medema RH, Hoeijmakers JH, Mullenders LH, Vermeulen W, Marteijn JA (2015) The core spliceosome as target and effector of non-canonical ATM signalling. *Nature* 523: 53–58
- Walz S, Lorenzin F, Morton J, Wiese KE, von Eyss B, Herold S, Rycak L, Dumay-Odelot H, Karim S, Bartkuhn N, Roels F, Wüstefeld T, Fischer M, Teichmann M, Zender L, Wei CL, Sansom O, Wolf E, Eilers M (2014) Activation and repression by oncogenic MYC shape tumour-specific gene expression profiles. *Nature* 511: 483–487

- Wang X, Cunningham M, Zhang X, Tokarz S, Laraway B, Troxell M, Sears RC (2011) Phosphorylation regulates c-Myc's oncogenic activity in the mammary gland. *Can Res* 71: 925–936
- Weber M, Davies JJ, Wittig D, Oakeley EJ, Haase M, Lam WL, Schubeler D (2005) Chromosome-wide and promoter-specific analyses identify sites of differential DNA methylation in normal and transformed human cells. *Nat Genet* 37: 853–862
- Welcker M, Orian A, Jin J, Grim JA, Harper JW, Eisenman RN, Clurman BE (2004) The Fbw7 tumor suppressor regulates glycogen synthase kinase 3 phosphorylation-dependent c-Myc protein degradation. *Proc Natl Acad Sci USA* 101: 9085–9090
- West MJ, Stoneley M, Willis AE (1998) Translational induction of the c-myc oncogene via activation of the FRAP/TOR signalling pathway. *Oncogene* 17: 769–780
- van de Wetering M, Sancho E, Verweij C, de Lau W, Oving I, Hurlstone A, van der Horn K, Batlle E, Coudreuse D, Haramis AP, Tjon-Pon-Fong M, Moerer P, van den Born M, Soete G, Pals S, Eilers M, Medema R, Clevers H (2002). The β -catenin/TCF4 complex controls the proliferation/differentiation switch in colon epithelium through c-MYC-mediated repression of p21CIP1/WAF1. *Cell* 111: 241–250
- Wiegner A, Uthe FW, Jamieson T, Ruoss Y, Hüttenrauch M, Küspert M, Pfann C, Nixon C, Herold S, Walz S, Taranets L, Germer CT, Rosenwald A, Sansom OJ, Eilers M (2015) Targeting translation initiation bypasses signaling crosstalk mechanisms that maintain high MYC levels in colorectal cancer. *Cancer Discov* 5: 768–781
- Wise DR, DeBerardinis RJ, Mancuso A, Sayed N, Zhang XY, Pfeiffer HK, Nissim I, Daikhin E, Yudkoff M, McMahon SB, Thompson CB (2008) Myc regulates a transcriptional program that stimulates mitochondrial glutaminolysis and leads to glutamine addiction. *Proc Natl Acad Sci USA* 105: 18782–18787
- Wolf E, Lin CY, Eilers M, Levens DL (2014) Taming of the beast: shaping Myc-dependent amplification. *Trends Cell Biol* 25: 241–248
- Xiang Y, Stine ZE, Xia J, Lu Y, O'Connor RS, Altman BJ, Hsieh AL, Gouw AM, Thomas AG, Gao P, Sun L, Song L, Yan B, Slusher BS, Zhuo J, Ooi LL, Lee CG, Mancuso A, McCallion AS, Le A et al (2015) Targeted inhibition of tumor-specific glutaminase diminishes cell-autonomous tumorigenesis. *J Clin Invest* 125: 2293–2306
- Xu IM, Lai RK, Lin SH, Tse AP, Chiu DK, Koh HY, Law CT, Wong CM, Cai Z, Wong CC, Ng IO (2016) Transketolase counteracts oxidative stress to drive cancer development. *Proc Natl Acad Sci USA* 113: E725–E734
- Yuneva M, Zamboni N, Oefner P, Sachidanandam R, Lazebnik Y (2007) Deficiency in glutamine but not glucose induces MYC-dependent apoptosis in human cells. *J Cell Biol* 178: 93–105
- Yuneva MO, Fan TW, Allen TD, Higashi RM, Ferraris DV, Tsukamoto T, Matés JM, Alonso FJ, Wang C, Seo Y, Chen X, Bishop JM (2012) The metabolic profile of tumors depends on both the responsible genetic lesion and tissue type. *Cell Metab* 15: 157–170
- Zheng M, Wang YH, Wu XN, Wu SQ, Lu BJ, Dong MQ, Zhang H, Sun P, Lin SC, Guan KL, Han J (2011) Inactivation of Rheb by PRAK-mediated phosphorylation is essential for energy-depletion-induced suppression of mTORC1. *Nat Cell Biol* 13: 263–272